Coronal and Stellar Mass Ejections
Proceedings IAU Symposium No. 226, 2005
K. P. Dere, J. Wang & Y. Yan, eds.

doi:10.1017/S1743921305000116

Flare-induced coronal disturbances observed with Norikura "NOGIS" coronagraph

K. Hori[1], K. Ichimoto[2], T. Sakurai[2], I. Sano[2], and Y. Nishino[2]

[1]Hiraiso Solar Observatory, National Institute of Information and Communications Technology, 3601 Isozaki, Hitachinaka, Ibaraki 311-1202, Japan
email: hori@nict.go.jp

[2]National Astronomical Observatory, National Institutes of Natural Sciences, 2-21-1 Ohsawa, Mitaka, Tokyo 181-8588, Japan

Abstract. A 2-dimensional Doppler coronagraph "NOGIS" (NOrikura Green-line Imaging System) at the Norikura Solar Observatory, NAOJ, is a unique imaging system that can provide both intensity and Doppler velocity of 2 MK plasma from the green coronal line emission λ5303 Å of Fe XIV. We present the first detection of a CME onset by NOGIS. The event was originally induced by a C9.1 confined flare that occurred on 2003 June 1 at an active region NOAA #10365 near the limb. This flare triggered a filament eruption in AR 10365, which later evolved into a partial halo CME as well as an M6.5 flare at the same AR 10365 on 2003 June 2. The CME originated in a complex of two neighboring magnetic flux systems across the solar equator: AR 10365 and a bundle of face-on tall coronal loops. NOGIS observed i) a density enhancement in between the two flux systems in the early phase, ii) a blue-shifted bubble and jet that later appeared as (a part of) the CME, and iii) a red-shifted wave that triggered a periodic fluctuations in Doppler shifts in the face-on loops. These features are crucial to understand unsolved problems on a CME initiation (e.g., mass supply, magnetic configuration, and trigger mechanism) and on coronal loop oscillations (e.g., trigger and damping mechanisms). We stress a possibility that interaction between separatrices of the two flux systems played a key role on our event.

Keywords. Sun: corona, flares, coronal mass ejections (CMEs), oscillations

1. Introduction

The green coronal line λ5303 Å of Fe XIV (2 MK formation temperature) is important to diagnose various coronal disturbances such as coronal waves or periodic oscillations. Spectroscopic observation is useful to get Doppler information with a high time resolution, although spatial information is limited to 1-dimensional along the slit (e.g., Koutchmy et al. 1983; Tsubaki 1988). The Fe XIV line is also used for 2-dimensional imaging observations such as the LASCO C1 coronagraph on the SOHO spacecraft (1.1–3 Rs with a pixel resolution of 5.6″), the Mirror Coronagraph for Argentina (MICA, 1.05–2 Rs with 3.7″/pix), and the Solar Eclipse Corona Imaging System (SECIS, 4.07″/pix) for the total eclipse. These instruments can monitor global coronal disturbances but Doppler information has not been available so far.

The intensity and Doppler imaging observation with the 2-dimensional Doppler coronagraph, NOGIS started in 1997 at the Norikura Solar Observatory, NAOJ (Ichimoto et al. 1999). The Doppler images (Dopplergrams) are constructed by subtracting a $\lambda - 0.45$ Å image from a $\lambda + 0.45$ Å image, which can provide the line-of-sight velocity up to $\pm$ 25 km s^{-1} with an accuracy of 0.6 km s^{-1}. Hence, the target phenomena suitable for NOGIS are coronal waves and flows, rather than fast ejections. NOGIS has a field of view of 2000 $\times$ 2000 pixels in a full frame mode and a spatial resolution of 1.84″ in a partial frame mode. Time resolution is reduced to 40 sec to increase S/N.

On 2003 June 1–2, NOGIS continuously observed a birth place of a CME that originated in a complex of two neighboring magnetic flux systems across the solar equator; a flare-productive active region, NOAA #10365, and a bundle of face-on coronal loops overarching a quiescent filament. By combining optical, EUV, and radio data, Hori et al.(2005) reported this event in detail with a scenario that can explain the whole observed evolution. Here we present an outline of Hori et al. (2005). We briefly discuss a propagating wave that was detected in Doppler shifts but not in intensity variations.

2. Event Overview

The huge coronal disturbances were observed above the west limb, in association with two limb flares that successively occurred at AR 10365. In Figure 1 (d), the GOES soft X-ray light curves of the two flares are shown with a solid line (1.0–8.0 Å) and a dashed line (0.5–4.0 Å). The two vertical dashed lines in Figure 1 indicate the start time of each flare; a C9.1 flare from 23:23 UT on June 1 and an M6.5 flare from 00:07 UT on June 2. The first flare was less eruptive while the second flare was associated with metric Type-II and -IV bursts, and a partial halo CME. According to TRACE 195Å (1.6 MK) images, the C9.1 flare activated a filament in AR 10365. Although the filament started to erupt with a mean plane-of-sky speed of 64 km s^{-1}, the eruption seems to have stagnated at 0.04 Rs above the limb. The height-time profile of the filament is given with asterisks in panel (d). After 15 min TRACE data gap (indicated by an arrow in panel (d)), the filament again started to erupt at 23:46 UT with a velocity of ∼67 km s^{-1} during the decay phase of the C9.1 flare. This eruption (or an associated disturbance) appeared in the NOGIS field-of-view from 00:05 UT as an expanding dark bubble (or a less dense region at 2 MK), whose height-time profile is shown with triangles in panel (d).

In Figure 1, the first and second panels show time slices of NOGIS Dopplergrams (a) and intensity maps (b) at a height of 0.15 Rs from the west limb. The vertical axes show the heliographic latitude in degree and the horizontal axes show the time in UT for the same period as in panels (c) and (d). White means red-shifts (a) or intensity (density) enhancement (b), while black means blue-shifts (a) or intensity decrease (b). In diagram (a), the color is normalized to the line-of-sight velocity of ±5.5 km s^{-1}. These diagrams show coronal disturbances propagating in north-south direction within or above two neighboring magnetic flux systems; a bundle of face-on coronal loops (N20–S05) and AR 10365 (S05–S29). Before the start of the two flares, NOGIS observed a formation of dense, 2 MK region in the space bounded between AR 10365 and the southern legs of the face-on loop system. The bright horizontal bands in panel (b) correspond to a slice of the dense region. According to NOGIS radial slices (not shown), this dense region slowly moved upward, apparently tracing EUV elongated structures standing within ±10° in latitude. In panel (c), from the top to the bottom, the plots in different colors show time evolutions of the maximum value in NOGIS intensity slices at heights of 0.08, 0.1, 0.13, 0.15, and 0.18 Rs from the west limb. As clearly seen in the lowest slice (black line), the coronal intensity above the limb peaked and then turned to decrease a few minutes prior to the start time of each flare.

As the filament erupted from AR 10365, the height of the outermost part of AR 10365 grew upward in NOGIS intensity images. The dark bubble mentioned above started to expand from the boundary of the growing AR 10365 and the overlying dense region when the two regions came into contact (00:05 UT). In Figure 1 panel (b), the cone-shaped weak dimming appearing from the latitudinal range of S7.5–S12.5 corresponds to the region swept by the bubble. From NOGIS radial slices (not shown), we confirmed that the bubble expanded both inward and outward with a projected speed of ∼140 km s^{-1}.

https://doi.org/10.1017/S1743921305000116 Published online by Cambridge University Press

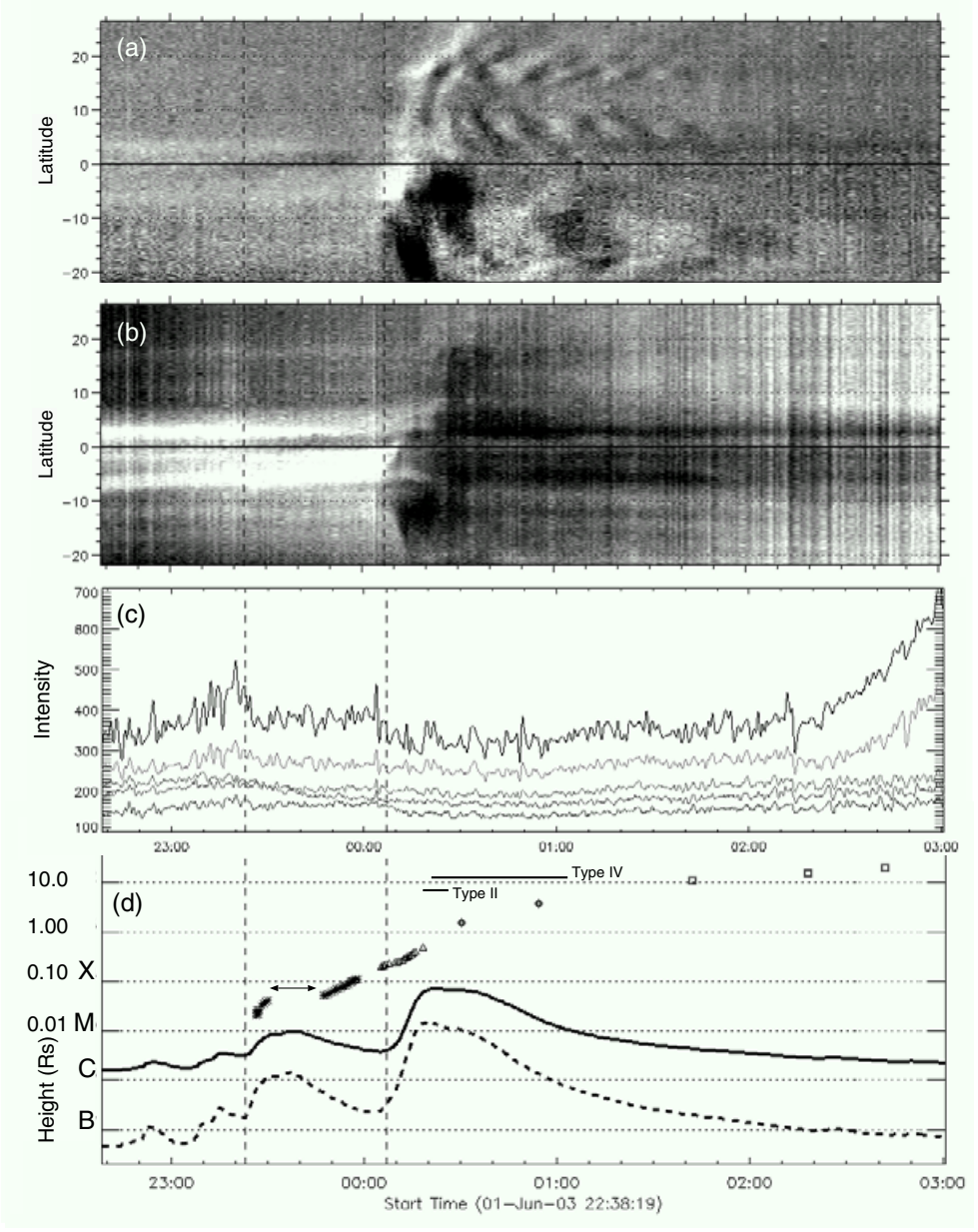

Figure 1. Time slices of NOGIS Dopplergrams (a) and intensity maps (b) at a height of 0.15 Rs from the west limb. The vertical axes show the heliographic latitude in degree. (c) From the top to the bottom, time profiles of the maximum intensity in the NOGIS time slices at heights of 0.08, 0.1, 0.13, 0.15, and 0.18 Rs from the west limb (in arbitrary scale). (d) Top: the height-time plots for the filament observed by TRACE (asterisks, the arrow indicates the period of a data gap), the expanding bubble observed by NOGIS (triangles), and the CME leading front observed by LASCO C2 (diamonds) and C3 (squares). Bottom: Time profiles of GOES 10 X-ray flux in 1.0–8.0 Å (thick solid line) and 0.5–4.0 Å (thick dashed line). All horizontal axes show the time in UT for the same period. The vertical dotted lines indicate the start time of two GOES flares; C9.1 (23:23–23:37–23:48 UT on June 1) and M6.5 (00:07–00:22–00:43 UT on June 2). The two horizontal bars indicate the periods of the metric Type-II (00:19–00:26) and -IV (00:20–01:03) from Culgoora.

https://doi.org/10.1017/S1743921305000116 Published online by Cambridge University Press

When the downward edge of the bubble arrived at the lower part of AR 10365 (00:10 UT), a blue-shifted jet was ejected upward with a velocity of ∼400 km s^{-1} from the interface of the two neighboring magnetic flux systems (S05). The jet soon overtook the preceding upward front of the bubble, pushed it from its behind, and accelerated it to ∼360 km s^{-1}. The impulsive phase of the second flare (M6.5) also started at 00:10 UT in AR 10365 (S08), which was defined by 17 GHz radiation from Nobeyama radioheliograph.

The collision of the two dense regions also produced a red-shifted velocity disturbance. In Figure 1 panel (a), the white arc appearing around S05 at 00:05 UT together with the cone-shaped dimming in panel (b) suggests that the disturbance propagated northward with a velocity of $>$ 1000 km s^{-1}, which is much faster than the projected expansion speed of the bubble. In the northern hemisphere, the disturbance pushed the face-on loop system anti-earthward and triggered damping oscillations in Doppler shifts among the adjacent loops within the system (the zebra pattern in panel (a)). The oscillations continued over 100 minutes with amplitudes of $< \pm 5$ km s^{-1} and periods in the range of 8–16 min.

The upward front of the bubble blew off the overlying dense region northward and extended toward the face-on loop system in the northern hemisphere (see the expansion of the dimming region in Figure 1 panel (b)). After the passage of the bubble in the NOGIS field-of-view, a partial halo CME appeared above the west limb that had a mean plane-of-sky speed of ∼1500 km s^{-1} (or an acceleration of ∼ 30 m s^{-2}). In Figure 1 panel (d), the height of the CME leading edge estimated from LASCO C2 and C3 images are plotted with diamonds and squares, respectively. The CME had an angular extent covering the latitudinal range of the two neighboring magnetic flux systems. The face-on loop system apparently remained at the same place, forming a cusp on its top.

3. Discussion

Using NOGIS, we observed huge coronal disturbances that were produced by a combined activity of two neighboring magnetic flux systems. The observed features (e.g., an expanding bubble, a propagating wave, and a jet) suggest that the two flux systems interacted (or reconnected) each other at the intersection of their magnetic separatrices (Beveridge, Priest, and Brown 2002). In between the two flux systems, 2 MK plasmas originated in the low corona had been accumulated since early phase. Through this dense region, the interaction was presumably triggered by a filament eruption that was induced by a C9.1 flare. The filament eruption resulted in a partial halo CME, an M6.5 flare, and coronal loop oscillations. The accumulated plasmas were blown off by the expanding bubble and thus (partially) contributed to the CME mass.

In our event, the propagating wave, or a red-shifted fast velocity disturbance, triggered damping oscillations in Doppler shifts among face-on coronal loops. Note that the wave was produced in the proximity of separatrices, which is a key to excite coronal loop oscillations as pointed by Schrijver and Brown (2000). On the basis of TRACE oscillation events (e.g., Aschwanden et al. 1999), Nakariakov (2003) described a flare-generated blast wave (fast-mode magnetoacoustic wave) as a possible excitation mechanism of kink oscillations of coronal loops (Figure 2, top). Hudson & Warmuth (2004) supports this idea considering a strong association of TRACE oscillation events with type II bursts and their temporal relationship. In our event, however, the wave was generated a few minutes earlier than the start time of the M6.5 flare (as well as the flare associated metric Type II burst). The M6.5 flare was not a generator of the wave. Instead, the wave might have induced the flare (Hori et al. 2005). Therefore, we consider another scenario that includes the role of magnetic separatrices (Figure 2 bottom). As the disturbance did not appear in

https://doi.org/10.1017/S1743921305000116 Published online by Cambridge University Press

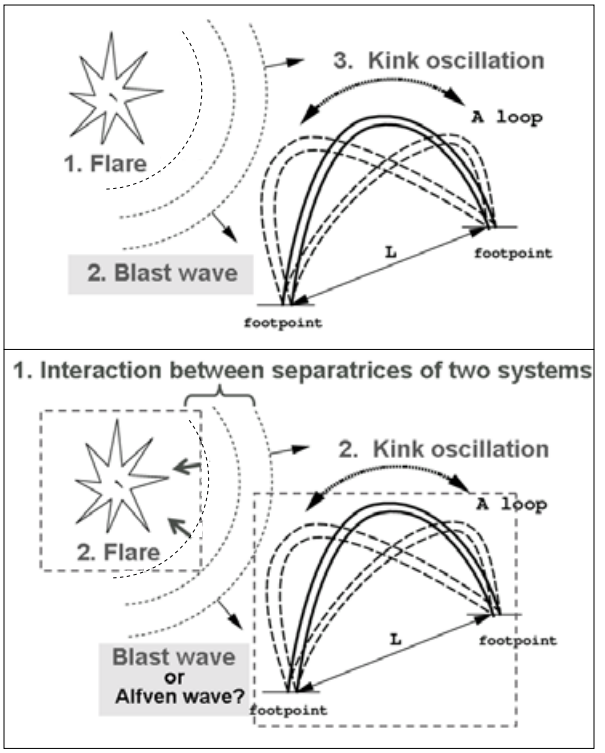

Figure 2. A possible mechanism for excitation of kink oscillations of coronal loops. Top: A flare-excited (#1) coronal blast wave (#2) may excite oscillations (#3) in a nearby flux system. After Nakariakov (2003) Bottom: An interaction between separatrices (#1) may excite flare (#2) and oscillations (#2) in each system.

intensity images (compare panels (a) and (b) in Figure 1), it might be an incompressible Alfvén wave, rather than a blast wave. It is, however, still possible that the oscillation in intensity (density) variations was too weak to be detected by NOGIS.

From the NOGIS observations, we learn the importance of ground-based imaging spectroscopy using visible lines for diagnosis of global coronal disturbances.

References

Aschwanden, M.J., Fletcher, L., Schrijver, C.J., Alexander, D. 1999, *ApJ* 520, 880

Beveridge, C., Priest, E. R., Brown, D. S. 2002, *Sol.Phys.* 209, 333

Hori, K., Ichimoto, K., Sakurai, T., Sano, I., Nishino, Y. 2005, *ApJ* 618, 1001.

Hudson, H.S., Warmuth, A. 2004, *ApJ* (Letters) 614, 85

Ichimoto, K., Noguchi, M., Tanaka, N., Kumagai, K., Shinoda, K., Nishino, T., Fukuda, T., Sakurai, T. 1999, *pasj* 51, 383

Koutchmy, S., Zhugzhda, Ia, D., Locans, V. 1983, *Sol.Phys.* 120, 185

Nakariakov, T 2003, in: B.N. Dwivedi (ed), *Dynamic Sun* (Cambridge University Press), pp.314-334

Schrijver, C.J., Brown, D.S. 2000, *ApJ* (Letters) 537, 69

Tsubaki, T 1988, in:Solar and stellar coronal structure and dynamics, Proceedings of the 9th Sacramento Peak Summer Symposium, pp.140-149

https://doi.org/10.1017/S1743921305000116 Published online by Cambridge University Press

Discussion

KOUTCHMY: Before the flare of June 1-2 you observed a density enhancement and after the flare you observed a dimming. Would you suggest this is due to a mass loss or can you explain this observation in term of temperature changes? (assuming that the mass of the CME is provided by the filament.)

HORI: That's a good question. We actually discussed it very seriously. In our event the CME occurred in between the two flux systems and both regions showed the dimming; not only the flare region but also a relatively cold region where the kink oscillation was observed. If the dimming was due to a temperature effect, we expect that only the hot region might become dark. Thus we concluded that this was due to the mass loss, i.e, the CME.

JIE ZHANG: Could you say something about the instrument, the quality, say, how many CME are observed per year?

HORI: The quality of the observation depends on the weather at the top of the Norikura Mountain. The event which I showed you was the clearest example. I do not know the exact number of the CMEs observed so far.

GOPALSWARY : Comment: You mentioned that this is the first detection of CME onset in coronal green line. However, a large number of coronal green line transients were observed and studied in the seventies. (De Mastus et al. 1971).

HORI: Yes. But there was no 2D Doppler observations in coronal green line before NOGIS (Dr. Koutchmy answered).

https://doi.org/10.1017/S1743921305000116 Published online by Cambridge University Press